

ON VARIATIONAL DYNAMICS IN REDSHIFT SPACE

INGA M. SCHMOLDT AND PRASENJIT SAHA

Department of Physics (Astrophysics), Oxford University, Keble Road, Oxford OX1 3RH, UK

Draft version September 17, 2018

ABSTRACT

Peebles (1989) showed that in the gravitational instability picture galaxy orbits can be traced back in time from a knowledge of their current positions, via a variational principle. We modify this variational principle so that galaxy redshifts can be input instead of distances, thereby recovering the distances. As a test problem, we apply the new method to a Local Group model. We infer $M = 4$ to $8 \times 10^{12} M_{\odot}$ depending on cosmology, implying that the dynamics of the outlying Local Group dwarves are consistent with the timing argument. Some algorithmic issues need to be addressed before the method can be applied to recover nonlinear evolution from large redshift surveys, but there are no more difficulties in principle.

Subject headings: large-scale structure of universe – galaxies: distances and redshifts – Local Group

1. INTRODUCTION

Phase space is six-dimensional and therefore six numbers for each particle will specify the dynamics completely. The standard approach is to define initial conditions as six numbers (positions and velocities in three dimensions) and integrate those forward in time. This is the usual N -body approach to the problem.

Alternatively, it is not necessary to define those six numbers at only one time. It is equally well possible to split them, such that three numbers will be known at an initial time, and three at a final time, where the former are derived from physical arguments about the initial state, and the latter are provided by data on the current state of the system. This is the boundary value approach.

The usual boundary value for structure formation by hierarchical clustering at initial times is the gravitational instability requirement that initial peculiar velocities must vanish: therefore, it is possible to express the orbits as a sum of growing modes. This is what perturbation theory is designed to do, and linear perturbation theory and its extension, the Zel'dovich approximation are in wide use. However, as structure formation is non-linear on small scales, a non-linear formalism would be more useful. Non-linear perturbation theory exists (e.g. Nusser and Dekel (1993), Gramann (1993a), Gramann (1993b), Buchert and Ehlers (1993)) but is very complicated and has convergence problems, i.e. the dynamics at early times can be fitted to a high accuracy only at the expense of a good fit at later times.

A different method (cf Peebles (1989)) of addressing the boundary value problem is to use the variational principle. The basic method is to start with a parameterisation of the orbits which satisfies the boundary conditions and then adjust the parameters until a stationary point of the action is found. (A variant, suggested by Gialvalisco et al. 1993 and implemented by Susperregi and Binney (1994), parameterises the density and velocity fields rather than the orbits.) This may seem like perturbation theory because it is a method which attempts to get better and better approximations of galaxy orbits but there are important differences. The main one is that perturbation

theory attempts to fit early times even at the expense of accuracy at later times, whereas the variational principle spreads out the errors more uniformly over all times. The variational principle is also algorithmically more straightforward to do to higher orders.

The main disadvantage of Peebles' original method is that it requires the input of distances to recover redshifts. Redshifts, however, are easy to measure, whereas distances are not. We therefore change to recovering distances from redshifts. The recent nearly all-sky redshift surveys QDOT and PSC z provide a strong motivation for variational methods in redshift space. Shaya, Peebles, and Tully (1993) and Shaya, Peebles, and Tully (1995) have pointed out that this could be achieved by treating the distance boundary condition as a parameter and fitting that until the recovered redshifts agree with the measured ones. Another approach is to modify the variational principle until the boundary conditions are of the desired form. We take such an approach and so does Whiting (1998) but the details in his treatment differ from ours. The attractive feature of this approach is that it only requires small modifications of Peebles' elegant original method.

In this paper we develop a redshift space variational method, apply it to a small system — the Local Group —, and point out the algorithmic problems that need to be solved to extend to larger systems.

Various aspects of the Local Group dynamics have been studied by Peebles (1989), Peebles (1990), Peebles (1994), and Dunn and Laflamme (1993). The new feature of our analysis is that we attempt to constrain the masses of the Milky Way, M31, and an underlying distribution of unclustered matter by using a likelihood approach.

Two points need to be made about these variational methods in general: Firstly, the true solutions of the variational action need not be a minimum even though the colloquial use of 'least action' has stuck (cf Peebles (1990)). Secondly, the equations solved are the same as for N -body integration, only the approximations used to solve them are different. In neither of the two approaches do particles have to be galaxies — they may well be samplers of some underlying distribution function and as Branchini

and Carlberg (1994) and Dunn and Laffamme (1995) have pointed out, applying the variational method using galaxies only, neglecting biasing and unclustered matter, leads to wrong results.

2. FORMULATION

Orbits of galaxies follow equations of motion of the form

$$\frac{d}{dt}(a^2\dot{\mathbf{x}}) = -\frac{\partial\Phi}{\partial\mathbf{x}}, \quad (1)$$

where \mathbf{x} are some comoving coordinates, and $a(t)$ is the scale factor of the universe. These equations are derivable from a stationary action, $\delta S = 0$, subject to some boundary conditions. In this work, we will distinguish between two different actions and different sets of boundary conditions leading to the same equations of motion.

2.1. Two Kinds of Boundary Condition

For simplicity, let x be one-dimensional in this subsection. Then the two cases are:

- the ‘real space’ case, where the boundary conditions are $a^2\dot{x} = 0$ at $t = 0$ (i.e., initial peculiar velocities zero) and $\delta x = 0$ at $t = 1$ (i.e., present positions fixed) with the action given by

$$S = \int_0^1 L dt, \text{ where } L = \frac{1}{2}a^2\dot{x}^2 - \Phi(x) \quad (2)$$

This is the action and the boundary conditions first proposed by Peebles (1989).

- the ‘redshift space’ case, where the initial boundary condition remains the same and the final one becomes $\dot{a}\delta x + a\delta\dot{x} = 0$ at $t = 1$ (i.e. present redshifts are fixed). The new boundary conditions will still lead to the same equations of motion if we change the action to

$$S = \int_0^1 (L - \dot{G}) dt, \text{ where } G = a^2x\dot{x} + \frac{1}{2}a\dot{a}x^2 \quad (3)$$

and L remains the same. Whiting (1998) describes more general transformations of this type.

The standard method for finding an orbit that will keep the action stationary and therefore is a solution to the equations of motion consists of formulating a parametric expression for the coordinates x which satisfies the boundary conditions and adjusting the parameters to make the action stationary. For the real space case, we choose the expression

$$x = \sum_{n=1}^N C_n f_n(t), \quad (4)$$

where C_n are a series of N coefficients and $f_n(t)$ is a temporal basis function. For the redshift space case,

$$x = \frac{cz}{\dot{a}(1)} + \sum_{n=1}^N C_n g_n(t) \quad (5)$$

To ensure that the boundary conditions are fulfilled, the basis functions have to satisfy

$$\begin{aligned} f_n(1) &= 0 \\ g_1(t) &= f_1(t) - \frac{\dot{f}_1(1)}{\dot{a}(1)}, \quad g_{n>1}(t) = f_n(t) \end{aligned} \quad (6)$$

A good choice for f_n is $(1 - D(t))^n$, where $D(t)$ is the growth factor from linear theory; this was proposed by Giavalisco et al. 1993. In this case, for $N = 1$ the variational method reduces to linear theory. But all that is essential is that linear theory should be followed as $t \rightarrow 0$. So, other choices such as $f_n = (1 - t^{2/3})^n$ are also possible.

2.2. Equations for Stationary Action

The real three-dimensional problem is a combination of the two types of boundary conditions. Because of the way in which we choose coordinate systems, the real space treatment can be used for the first two dimensions (x, y) of each orbit and only the third dimension (z) will have to be treated in redshift space. We will refer to axes by their dimension rather than by a x, y , or z in order to prevent confusion between the third dimension and the symbol used for redshifts.

One coordinate system is assigned to each object and all coordinate systems share a common origin. This origin is the point from which a comoving observer would measure the objects’ redshifts. It is important to note that, although the objects move, their coordinate frames do not. By pointing the 3-axis of each frame towards the current galactic coordinates l, b of the object associated with it, we ensure that the radial velocity is along one axis only. Therefore, the redshift space treatment will have to be applied only to that axis. With this orientation, the 3-coordinate of each object is cz_i ($cz_i = \dot{a}x_{i3} + a\dot{x}_{i3}$), where z_i is the ‘comoving’ redshift, i.e. the redshift measured by an observer who is at rest with respect to the microwave background. The 1,2-coordinates at $t = 1$ are $x_{i1} = 0, x_{i2} = 0$, so the current positions are completely specified and real space treatment can be applied.

In these coordinates, the parametric expansion of the position \mathbf{x} of an object i becomes

$$x_{i(1,2)} = \sum_{n=1}^N C_{i(1,2),n} f_n(t) \quad (7)$$

$$x_{i(3)} = \frac{cz}{\dot{a}(1)} + \sum_{n=1}^N C_{i(3),n} g_n(t) \quad (8)$$

and the full action is $\int_0^1 (L - \dot{G}) dt$, where L and G are

$$L = \frac{1}{2} \sum_i m_i a \dot{\mathbf{x}}_i^2 - \frac{1}{2} \ddot{a} a \sum_i m_i \mathbf{x}_i^2 + \frac{1}{a} \sum_{i,j} \frac{m_i m_j}{|\mathbf{x}_i - \mathbf{x}_j|^{1/2}} - \Phi_{\text{tidal}} \quad (9)$$

and

$$G = \sum_i m_i \left(a^2 x_{i(3)} \dot{x}_{i(3)} + \frac{1}{2} a \dot{a} x_{i(3)}^2 \right). \quad (10)$$

The first term in equation 9 describes the total kinetic energy, the second term is an acceleration caused by the fact that the coordinate system is expanding at a rate $a(t)$,

and the third term describes the gravitational interaction between members of the group of objects. Φ_{tidal} represents the tidal potential caused by the influence of objects external to the region considered. Note that introducing a homogeneous mass distribution into the system is very easy since it will only rescale the second term.

Inserting the equations 9 and 10 into the action S and taking the gradient with respect to the C_i leads to

$$\left[\int_0^1 a^2 \dot{f}_m \dot{f}_n dt \right] C_{i(1,2),n} = \int_0^1 \frac{f_n}{a} \sum m_i m_j \nabla_{i(1,2)} |\mathbf{x}_i - \mathbf{x}_j|^{-1} - \frac{\partial \Phi_{\text{tidal}}}{\partial C_{i(1,2)}} \quad (11)$$

and

$$\begin{aligned} & \frac{\dot{f}_1(1)^2}{\dot{a}(1)} C_{i(3),1} + \left[\int_0^1 a^2 \dot{g}_m \dot{g}_n dt \right] C_{i(3),n} \\ & + \int_0^1 \dot{a} a g_n dt \frac{cz_i}{\dot{a}(1)} = \\ & \int \frac{g_n}{a} \sum m_i m_j \nabla_{i(3)} |\mathbf{x}_i - \mathbf{x}_j|^{-1} - \frac{\partial \Phi_{\text{tidal}}}{\partial C_{i(3)}} \quad (12) \end{aligned}$$

To find the orbits which keep the action stationary, we now have to solve equations 11 and 12 for the spatial coefficients $C_{i,n}$. The standard method is to assume some initial coefficients, calculate the right hand sides, then solve the left hand sides for the coefficients and use the results to recalculate the right hand sides. Note that the left hand side integrals in equations 11 and 12 have to be done only once.

We have experimented with various procedures to help convergence, e.g. adding a stabilising term $\propto \left[\int \dot{a} a f_m f_n dt \right] C_{i,m}$ on both sides of the equation or scaling down some terms for early iterations and only slowly increasing them to their full value (cf Susperregi and Binney (1994), Giavalisco et al. 1993).

2.3. Units

It is convenient to define model units for time, mass, and length (tick, marble, and lap) which we keep scaleable with the age of the universe T_0 , since T_0 is not known. The units are given by

$$1 \text{ tick} = T_0 = 10 \kappa \text{ Ga} \quad (13)$$

and κ is the age of the universe in units of 10 Ga. We do not want the velocities to be scaleable, so we require $100 \text{ km/s} = 1 \text{ lap/tick}$ which leads to

$$1 \text{ lap} = 1.023 \kappa \text{ Mpc} \quad (14)$$

The assumption of a gravitational constant equal to unity as in the equations above leads to

$$1 \text{ marble} = 2.38 \cdot 10^{12} \kappa M_{\odot} \quad (15)$$

We therefore have a one-parameter family of models for different ages of the universe.

3. APPLICATION TO THE LOCAL GROUP

In this section we will apply the above formalism to a small group of galaxies, namely the Milky Way–M31 system and outlying Local Group dwarves, with external forces approximated by dipole and quadrupole tidal forces growing according to linear theory. Since distances to objects within this group are fairly well known, we can constrain the mass distribution by comparing the distances predicted by our method to the observed distances for a range of different mass distributions. We also test the effects of assuming different values for Ω_0 .

3.1. Formulation for the Local Group

The formalism is outlined in section 2, but for the Local Group there are two special considerations:

Firstly, the Milky Way has a special role. As explained above, each galaxy has its own coordinate system, and we take the current position of the Milky Way as the common origin. This origin is at rest with respect to the CMB and for $t \neq 1$ the Milky Way moves away from it. As the Milky Way's current position is fixed the real space treatment can be applied in all three dimensions.

Secondly, cosmology only influences the Local Group via tidal forces. Therefore, we can keep things simple by introducing the following complication: The integrals on the left hand sides of equations 11 and 12 are particularly simple to solve for $a(t) = t^{2/3}$, and we exploit this fact by setting $a(t) = t^{2/3}$ regardless of cosmologies. This $a(t)$ is only the scale factor of a convenient frame that we have chosen for the Local Group and which need not necessarily bear any relation to the real physical scale factor of the universe $a_{\text{phys}}(t)$ except at the boundaries

$$\begin{aligned} a(t \rightarrow 0) &= t^{2/3} \propto a_{\text{phys}}(t \rightarrow 0) \\ a(t = 1) &= 1 = a_{\text{phys}}(t = 1) \end{aligned} \quad (16)$$

For interactions between members of the group, the value of $a(t)$ does not matter. Only when calculating the influence of the tidal forces do we have to consider the relation between the two sets of comoving coordinates $\mathbf{x}_{\text{phys}} = \frac{a}{a_{\text{phys}}} \mathbf{x}$. The tidal potential then is

$$\Phi_{\text{tidal}} = \frac{D(t)}{a_{\text{phys}}} \left[\mathbf{d} \cdot \mathbf{x}_{\text{phys}} + \frac{1}{2} \mathbf{x}_{\text{phys}} \cdot \mathbf{Q} \cdot \mathbf{x}_{\text{phys}} \right] \quad (17)$$

where $D(t)$ is the growth rate of the density fluctuations, \mathbf{d} is the dipole and \mathbf{Q} is the quadrupole strength.

The quadrupole potential is taken from Raychaudhury and Lynden-Bell, (1989). The dipole is inferred indirectly from the Milky Way's known velocity with respect to the microwave background, in the following way. As the equations (11) and (12) are being solved for the orbits of all galaxies involved, we constantly monitor the development of the predicted velocity of the Milky Way. This velocity depends on the strength of the dipole. During the iterations, we fit that dipole strength such that the predicted velocity of the Milky Way agrees with the one measured by Kogut et al. 1993.

3.2. Finding Solutions in the Local Group

We model the Local Group as an ensemble of 13 galaxies with the mass of the system distributed between the Milky Way, M31, and some local unclustered matter ρ_{sm} . It is convenient to express this ρ_{sm} in units of the critical density, but it is important to note that it is only local and does not change the cosmology. The cosmological models have $\Lambda = 0$ and various Ω_0 . The ratio of masses of Milky Way and M31 is fixed at 2:3 and all dwarf galaxies are treated as test particles.

We select the dwarf galaxies by choosing all objects from the list of Local Group members (Hodge et al (1993)) which are more than 500 kpc away from both M31 and the Milky Way. This high distance is a necessary restriction because the orbits of nearby galaxies tend to be too dominated by the internal dynamics of the Milky Way–M31 system and are therefore difficult to reconstruct. Nearby galaxies might also be part of the system’s halo. The dwarf galaxies chosen, on the other hand, are generally not too sensitive to the mass ratio between M31 and the Milky Way because of their relatively great distance to that system. Distances (from Hodge et al (1993)) and redshifts (from the Nasa/IPAC Extragalactic Database) of all galaxies are listed in table 1. Note that these heliocentric redshifts are converted to CMB–centric redshifts to get the appropriate boundary conditions.

Galaxy	l deg	b deg	cz $\frac{\text{km}}{\text{s}}$	d_{obs} kpc	d_{model} (kpc/ κ)
M31	121.2	-21.6	-300	725	787
IC1613	129.8	-60.6	-234	765	498
WLM	75.9	-73.6	-116	940	1224
Sextans A	246.2	39.9	324	1300	1878
N3109	262.1	23.1	403	1260	1977
IC10	119.0	-3.3	-344	1250	1227
Pegasus	94.8	-43.5	-183	1800	1911
Sextans B	233.2	43.8	301	1300	2023
SagDIG	21.1	-16.3	-77	1150	1266
LGS 3	126.8	-40.9	-277	760	1220
EGB0427+63	144.7	10.5	-99	800	2069
N6822	25.3	-18.4	-57	540	1554

Table 1: Local Group Members; predicted distances are from the solution pictured in figure 1

In order to increase our chances of finding the right solutions among the many possible ones, we start the code with an initial guess by choosing the $C_{i,n} = 0$ except for

$$C_{i3,1} = d_{i_{\text{obs}}} - \frac{cz_i}{\dot{a}(1)}. \quad (18)$$

This produces an initial set of $\mathbf{x}_i(t)$ which fit the redshifts and measured distances (if 1 lap = 1 Mpc) but which are not solutions of the equations of motion. We therefore add an extra term to equations 11 and 12 to change them into something that the \mathbf{x}_i are solutions of. This term is then gradually removed from the equations during iteration.

Our current method always produces convergence of the coefficients, but does not do so in a very efficient way. In most cases, we need several hundred iterations to achieve convergence, where the main problem seems to be that some of the converging $C_{i,n}$ are caught in a cycle of two

values. We have tried to remedy this problem in a very crude way and were successful but only at a severe cost in iterations; this is one of the problems that will have to be solved in a more general way, before the code can be applied to large datasets.

We check our reconstructed \mathbf{x}_i by taking their values at $t = 0.01$ as the initial conditions of an N -body integration.

Figure 1 shows the variational orbits and N -body orbits for a system of a total mass of 3.10 marbles. For the mass distribution of table 1, the dipole acceleration inferred is 0.85 laps/tick² in the direction $l = 274^\circ$ and $b = 29^\circ$ (the direction is indistinguishable from Yahil, Tammann, and Sandage (1977)).

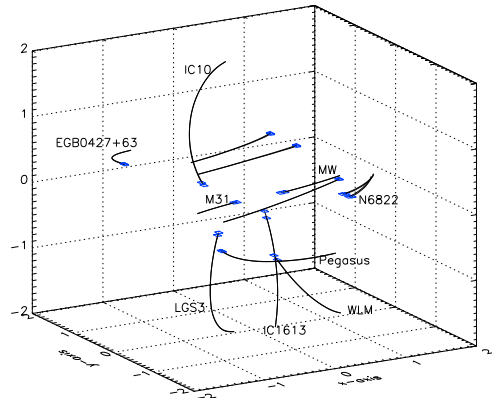


Figure 1. Variational and N -body orbits for $\Omega = 0.99$, $m_{\text{tot}} = 3.10$ marbles (no unclustered matter); squares indicate positions at $t = 1$; the scale is in comoving laps and the coordinate directions are $(\cos b \cos l, \cos b \sin l, \sin b)$. We have labelled as many of the galaxies as was possible without overcrowding the figure.

The last column of table 1 lists the predicted distances for this particular model. They are generally similar to the measured distances, which is not a trivial result, since as far as the mathematical formalism is concerned, the predicted distances are not even constrained to be positive. In fact, when trying to reconstruct the orbits of galaxies which are too close to M31 or the Milky Way, the code does produce negative distances. A typical example of this is Leo I (cf Zaritsky et al (1989)): the code is given a positive redshift but only finds approaching solutions. The only way to reconcile these two requirements is to put the dwarf galaxy on the other side of the Milky Way - which is what produces the negative distance. The reason for this is that nearby galaxies are too dominated by halo dynamics and we have not attempted to model the halo in any way. Hence our decision to exclude all the nearer dwarf galaxies.

3.3. Analysis of Local Group Solutions

To quantitatively analyse our results, we assign a likelihood to each set of solutions and therefore to each mass distribution. The following is very crude, but we decided to use it because it is well defined and uses plausible reasoning. The likelihood is calculated in the standard Bayesian fashion by assessing the probability of a set of solutions given the set of measured distances. We have to allow for the uncertainties associated with the measured

distances, and the fact that some of our solutions might simply be wrong (we call this the ‘outlier probability’). As we have no particular reason to believe that the uncertainties in d_{obs} are Gaussian, we use (for all galaxies except M31) the hatbox function

$$\text{hb}(x, a, b) = \begin{cases} (b - a)^{-1} & \text{if } a \leq x \leq b \\ 0 & \text{otherwise} \end{cases}$$

If the outlier probability is α and the uncertainty in d_{obs} is β then

$$\begin{aligned} \text{prob}(d_{\text{obs}}^i | d_{\text{model}}^i) &= \alpha \text{hb}(d_{\text{obs}}, \min(d_{\text{obs}}, \max(d_{\text{obs}})) \\ &+ (1 - \alpha) \text{hb}(d_{\text{obs}}^i, (1 - \beta)d_{\text{obs}}^i, (1 + \beta)d_{\text{obs}}^i) \end{aligned} \quad (19)$$

For M31 we take $\text{prob}(d_{\text{obs}}^i | d_{\text{model}}^i)$ to be Gaussian where the observed distance has an associated uncertainty of 5%.

Combining all galaxies, we have,

$$\text{prob}(\text{data} | \text{model}, \alpha, \beta) = \prod_i \text{prob}(d_{\text{obs}}^i | d_{\text{model}}^i, \alpha, \beta) \quad (20)$$

Since we do not know α or β , we marginalise by integrating over a plausible range of both with a suitable prior, i.e. we integrate over $0.1 \leq \alpha \leq 0.3$ with a flat prior and $0.1 \leq \beta \leq 0.3$ with a $1/\beta$ prior.

Figure 2 shows likelihood contours for two different values of Ω_0 .

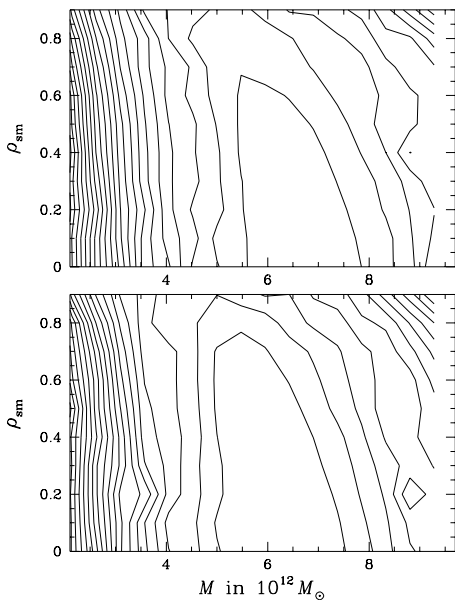


Figure 2. Likelihood contours for variational solutions associated with different mass distributions: above $\Omega = 0.4$, below $\Omega = 0.99$. In both cases, $\kappa = 1$. Contour levels differ by a factor of 10.

Masses are particularly high for low Ω_0 because the quadrupole force, which pulls the Milky Way and M31 apart is higher in those cosmologies and so we require more mass to keep the two galaxies at the same distance from each other.

The likelihood contours are dominated by M31: leaving one or more of the dwarf galaxies out of the likeli-

hood analysis does not make a lot of difference to the contours whereas leaving out M31 severely limits the statement that can be made about the mass of the system. In the $\Omega_0 = 0.99$ universe, for example, we can only say that the combined mass of the system is probably less than $9 \times 10^{12} M_{\odot}$.

Figure 3 shows the same contours as figure 2 but for the case of an older universe. The masses generally decrease in this case, because less mass is needed to produce the same results when gravitation works over a longer period in time.

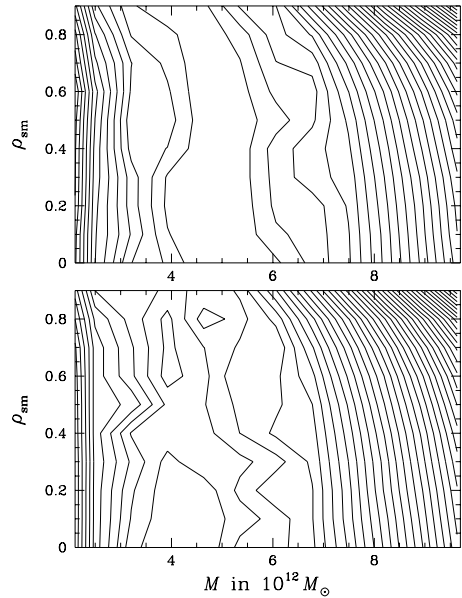


Figure 3. As for figure 2 but with $\kappa = 1.5$.

Both figure 2 and 3 were produced from a set of solutions using 8 basis functions. We experimented with different numbers of basis functions but the results remain the same.

Our results indicate that most of the physics are included in our model if not all of them. Hence we opted for a likelihood analysis. The analysis shows the system dominated by M31, which makes our model not so very different from the one used for the timing argument. However, if we leave M31 out of the analysis, the resulting contours are at least consistent with figures 2 and 3. There seems to be some slight preference for mass to cluster with the galaxies, but the contours are not really conclusive.

4. DISCUSSION

The N -body check proves that the code works and is ready to be extended to larger systems. The main problem with a system like the Local Group is the occurrence of multiple solutions. We have no guarantee that the solutions we find are the real ones, even if they fit all redshifts perfectly and predict distances which are not too far out from the measured ones. In fact, some tests suggests that at least for certain masses, several possible solutions are very close to each other so it is easy to pick the wrong one. This problem will not occur in larger systems, so they should in fact be easier to deal with.

In future work, two issues will need to be addressed: First, we need an approximate and more efficient way of doing the force calculations in equations 11 and 12. The direct sum that we have used needs to be replaced by a standard N -body method. Second, we need more efficient convergence. As mentioned above, the main difficulty lies in preventing the coefficients from finding two-cycles instead of fixed points of the iteration. A faster yet still robust method for dealing with this problem is needed.

Even when these problems are solved, the variational calculations will never have as many particles as N -body

simulations. The reason for pursuing this method is that unlike the N -body calculation, which can only reproduce the current state of the system in a statistical sense, the variational method can fit the current state exactly.

The authors would like to thank Alan Whiting and James Binney for many helpful comments and suggestions. I. S. acknowledges a PPARC studentship and an Oriel College graduate scholarship.

REFERENCES

- Branchini, E., Carlberg, R., ApJ 434,37 (1994)
 Buchert, T., Ehlers, J., 1993, MNRAS,264,275
 Dunn, A.M. and Laflamme, R. 1993, MNRAS, 426,865
 Dunn, A.M. and Laflamme, R. 1995, ApJ, 443, L1
 Giavalisco, Mancinelli, Mancinelli, and Yahil (1993) ,ApJ, 411,9
 Gramann, M. 1993a, ApJ, 405,449
 Gramann, M. 1993b, ApJ, 405,L47
 Hodge, P. 1993, Proceedings of V Canary Islands Winter School of Astrophysics, Ed. Sanchez, F., Munoz-Tunon, C., Cambridge University Press, ISBN 052149575X
 Kogut et al., ApJ, 419,1
 Nusser, A., Dekel, A., 1992, ApJ, 391, 443
 Peebles, P.J.E. 1989, ApJ, 344, L53
 Peebles, P.J.E. 1990, ApJ, 362,1
 Peebles, P.J.E. 1994, ApJ, 429,43
 Raychaudhury, S., Lynden-Bell, D., MNRAS, 240,195
 Shaya, Peebles, and Tully, Conf. Cosmic Velocity Fields (Paris, July 93)
 Shaya, Peebles, and Tully, ApJ, 454,15
 Susperregi, M., Binney, J. MNRAS 271,719 (1994)
 Whiting, A. B., ApJ, (submitted)
 Yahil, Tammann, and Sandage, 1977, ApJ, 217,903
 Zaritsky, D., Olszewski, W., Schommer, A.R., Peterson, R.C., and Aaronson, M. ApJ 345,759 1989